Title

Cell cycle regulation of dynein association with membranes modulates microtubule-based organelle transport.

Journal

The Journal of cell biology, 133(3)

ISSN

0021-9525

Authors

Niclas, J
Allan, VJ
Vale, RD

Publication Date

1996-05-01

DOI

10.1083/jcb.133.3.585

Peer reviewed

Cell Cycle Regulation of Dynein Association with Membranes Modulates Microtubule-based Organelle Transport

Joshua Niclas,* Viki J. Allan,§ and Ronald D. Vale*‡

*Departments of Pharmacology and Biochemistry and ‡The Howard Hughes Medical Institute, University of California, San Francisco, California 94143; and §School of Biological Sciences, University of Manchester, Manchester, M139PT United Kingdom

Abstract. Cytoplasmic dynein is a minus end–directed microtubule motor that performs distinct functions in interphase and mitosis. In interphase, dynein transports organelles along microtubules, whereas in metaphase this motor has been implicated in mitotic spindle formation and orientation as well as chromosome segregation. The manner in which dynein activity is regulated during the cell cycle, however, has not been resolved. In this study, we have examined the mechanism by which organelle transport is controlled by the cell cycle in extracts of *Xenopus laevis* eggs. Here, we show that photocleavage of the dynein heavy chain dramatically inhibits minus end–directed organelle transport and that purified dynein restores this motility, indicating that dynein is the predominant minus end–directed membrane motor in *Xenopus* egg extracts. By measuring the amount of dynein associated with isolated membranes, we find that cytoplasmic dynein and its activator dynactin detach from the membrane surface in metaphase extracts. The sevenfold decrease in membrane-associated dynein correlated well with the eightfold reduction in minus end–directed membrane transport observed in metaphase versus interphase extracts. Although dynein heavy or intermediate chain phosphorylation did not change in a cell cycle–dependent manner, the dynein light intermediate chain incorporated ~12-fold more radiolabeled phosphate in metaphase than in interphase extracts. These studies suggest that cell cycle–dependent phosphorylation of cytoplasmic dynein may regulate organelle transport by modulating the association of this motor with membranes.

A variety of membranous organelles in the cytoplasm are transported along a polarized microtubule array to specific destinations within the cell. The complexity of this membrane traffic must require precise means of regulating both the levels and directionality of such microtubule-based motility. Physiological regulation of organelle transport has been demonstrated most clearly in fish chromatophores, where a cAMP-dependent kinase pathway (Lynch et al., 1986*a*, *b*; Rozdzial and Haimo, 1986) is involved in the plus end–directed dispersion of pigment granules along microtubules. Conversely, dephosphorylation mediated by the phosphatase calcineurin (Thaler and Haimo, 1990) and an increase in intracellular Ca^{2+} (Kotz and McNiven, 1994) have been implicated in the minus end–directed aggregation of these particles. Phosphorylation may control organelle transport in other cells as well, since the protein phosphatase inhibitor okadaic acid enhances minus end–directed ER tubule transport in frog egg extracts (Allan, 1995), bidirectional transport in mammalian cells in culture (Hamm-Alvarez et al., 1993), and plus end–directed lytic granule movements in T cell extracts (McIlvain et al., 1994). In contrast, phosphorylation mediated by a $p34^{cdc2}$ kinase cascade suppresses organelle motility in metaphase frog egg extracts (Allan and Vale, 1991).

Protein motors, the ATP-hydrolyzing enzymes that power the movement of organelles on microtubules, represent likely targets for regulation of vesicle transport. The two best-studied organelle motors, dynein (Paschal et al., 1987; Paschal and Vallee, 1987) and kinesin (Brady, 1985; Vale et al., 1985), move membrane-bound compartments towards the minus ends (slow growing) (Schnapp and Reese, 1989; Schroer et al., 1989) and plus ends (fast growing) (Hollenbeck and Swanson, 1990; Rodionov et al., 1991) of microtubules, respectively. Both kinesin (Hollenbeck, 1993; Matthies et al., 1993; Okada et al., 1995) and dynein (Dillman and Pfister, 1994; Lin et al., 1994) are phosphorylated in cells, although the kinases involved and the functional consequences of such phosphorylation remain largely unresolved. Modulation of dynein and kinesin activity by phosphorylation, however, has been suggested by several studies. In the case of kinesin, specific phosphoisoforms were found to be selectively bound to membranes, and their levels were increased during neurite outgrowth after addition of NGF (Lee and Hollenbeck, 1995). For dynein, the heavy chain was observed to be less phosphor-

Address all correspondence to Dr. Ronald D. Vale, Department of Pharmacology, Box 0450, 513 Parnassus Ave., University of California, San Francisco, CA 94143 Tel.: (415) 476-6380. Fax: (415) 502-1391.

ylated on anterogradely moving vesicles in rat optic nerves compared with the total dynein pool, suggesting that dephosphorylation may inactivate dynein so that it could be carried by plus end–directed motors to the nerve terminal (Dillman and Pfister, 1994). In another study, okadaic acid was found to increase phosphorylation of the cytoplasmic dynein heavy chain as well as change the dynein immunofluorescence pattern from a vesicular staining to a more diffuse pattern (Lin et al., 1994).

Organelle transport may also be regulated by motor-associated factors, some of which have been purified or partially purified using in vitro assays (Schroer and Sheetz, 1991). The best-characterized activator is a multi-subunit factor called the dynactin complex which is required for dynein function in organelle motility (Gill et al., 1991) as well as during mitosis (Muhua et al., 1994; Plamann et al., 1994; Echeverri et al., 1996). The mechanism by which dynactin regulates dynein activity, however, remains unclear. Three kinesin-associated proteins have also been implicated in regulating organelle movement, since their phosphorylation levels increased concomitantly with a twofold increase in lytic granule movement along microtubules after okadaic acid treatment (McIlvain et al., 1994).

In this study, we have examined the mechanism by which organelle transport is regulated by the cell cycle in *Xenopus laevis* eggs. In previous work, metaphase-arrested egg extracts were shown to support 10-fold lower levels of bidirectional organelle motility compared with interphase extracts (Allan and Vale, 1991). This cell cycle regulation of organelle transport is consistent with an overall decrease in vesicular trafficking in the secretory and endocytic pathways in mitosis (Warren et al., 1983, 1984). Here, we have investigated whether the cell cycle regulation of organelle movement involves a change in either the force-generating activity of microtubule motors or the association of motor proteins with membranes. We show that cytoplasmic dynein is the predominant minus end organelle motor in *Xenopus* egg extracts and that cytoplasmic dynein and its activator dynactin detach from the membrane surface when interphase extracts are converted to a metaphase state. By measuring organelle motility in the same extracts, we find that the reduction in membrane-associated dynein correlates well with the decrease in minus end organelle transport in metaphase extracts. While cell cycle–dependent phosphorylation of the dynein heavy chain and the 85-kD intermediate chain was not observed, a substantial increase in the phosphorylation of the 65-kD dynein light intermediate chain was seen in metaphase compared with interphase extracts. These results suggest that dynein-based organelle transport is controlled by cell cycle–dependent phosphorylation events that regulate the attachment of dynein to intracellular membranes.

Materials and Methods

Xenopus Egg Extracts

Interphase extracts were prepared from electrically activated *Xenopus laevis* eggs (Murray, 1991) with the following modifications. Cycloheximide was used during the egg breakage step to inhibit cyclin synthesis and hence arrest the extract in the interphase state. Final extracts contained 1 mM DTT, 100 μg/ml cycloheximide, *Xenopus* protease inhibitors (10 μg/ml leupeptin, 10 μg/ml chymostatin, 10 μg/ml pepstatin, 10 μg/ml aprotinin), and 10 μg/ml cytochalasin B. Extracts, which were typically 80–100 mg/ml in protein concentration, were stored in liquid nitrogen. Metaphase extracts were made by treating interphase extracts with partially purified bacterially expressed cyclin Δ90 (0.13 mg/ml final concentration), a nondegradable form of cyclin B, for 45 min at 22°C, in the presence of an ATP-regenerating system (1 mM ATP, 1 mM $MgCl_2$, 7.5 mM creatine phosphate). Cyclin Δ90 maintains the extract in the mitotic state (Murray et al., 1989). Histone H1 kinase assays (Murray, 1991) were used to assess the cell cycle state of interphase and metaphase extracts.

UV Vanadate Photocleavage of Egg Extracts

Interphase crude extracts were supplemented with 2 mM ATP, 5 mM Mg-acetate, 2 mM DTT, and 20 μM sodium orthovanadate. 40-μl drops of extract on sheets of parafilm taped to aluminum foil on a flat layer of ice were irradiated for 1 h at a distance of 1 cm with UV light (366 nm) using a lamp (UVL-56 Blak-Ray; UVP, Inc., San Gabriel, CA). Although other studies have used norepinephrine to reduce and thereby inactivate the orthovanadate ion after irradiation (Schnapp and Reese, 1989; Schroer et al., 1989), we found that this compound inhibited organelle transport in *Xenopus* extracts. However, when orthovanadate was diluted to 8 μM in the motility assay, this concentration did not substantially inhibit organelle transport or minus end–directed bead movement and microtubule gliding. High speed supernatants and membrane samples used in microscope assays were made as described below.

Preparation of High Speed Supernatants and Membranes

Xenopus egg crude extract samples were diluted with 1 vol of acetate buffer (10 mM Hepes, pH 7.4, 100 mM K-acetate, 150 mM sucrose, 5 mM EGTA, 3 mM Mg-acetate) containing protease inhibitors (described above) and 1 mM DTT and then spun at 109,000 g_{max} for 30 min at 2°C in either a TLA 120.1 or TLA 100.4 rotor (Beckman Instruments, Inc., Fullerton, CA). High speed supernatants and membrane pellets were collected. The membrane pellets were resuspended in 3 vol of 2 M sucrose in acetate buffer and then layered above 2 M sucrose/acetate buffer and below 1.4 M and 0.25 M sucrose/acetate buffer cushions. The membranes were then isolated by flotation up to the 0.25 M/1.4 M sucrose interface by spinning at 260,000 g_{max} for 30 min in a TLS-55 rotor (Beckman Instruments, Inc.). These flotation gradients were designed to collect the majority of the membranes in the extract and to purify them away from contaminating nonmembranous dynein that cosedimented with the membranes during the first spin. Regarding dynein recovery, immunoblotting results indicated that 20–30% of dynein from the crude extracts was associated with the membrane fraction obtained by centrifugation (109,000 g_{max}; 30 min) through a 0.5-M sucrose cushion. When membranes were purified by the additional flotation step and subjected to immunoblotting, we estimate that half of the dynein was not recovered in the flotation.

Organelle and Bead Transport Assays

Organelle motility assays were performed in ~5-μl flow cells made from glass coverslips and slides spaced apart by two parallel strips of double-stick tape. Assays were done by pipetting samples sequentially into the flow cell in a 3-step process. (*1*) First, to polymerize an oriented microtubule array from centrosomes, 5 μl acetate buffer, 4 μl interphase frog egg high speed supernatant, 1 μl crude aster-forming surf clam (*Spisula solidissima*) egg extract (Palazzo et al., 1988, 1992) (gift from Robert Palazzo, Department of Physiology/Cell Biology, University of Kansas, Lawrence, KS) and 0.5 μl 20× ATP regeneration system were flowed into the chamber. (*2*) Once an astral array of microtubules was located, it was washed and stabilized with 30 μl acetate buffer containing 0.4 μM taxol and the ATP regeneration system. (*3*) Finally, the samples of high speed supernatants with added organelles or 0.2 μM carboxylated beads (Polysciences, Inc., Warrington, PA) and the ATP-regenerating system were introduced into the chamber. The movement of organelles or beads was then observed on a microscope (Axioplan; Carl Zeiss, Inc., Thornwood, NY) equipped with differential interference contrast optics, a 50 W or 100 W mercury arc lamp, and a ×63 1.4 NA Planapochromat objective. Images were detected using a camera (Newvicon; Hammatsu Photonics, Bridgewater, NJ); contrast enhancement and background subtraction were performed with an image processor (Argus 10; Hammatsu Photonics), and recordings made with a super VHS video tape recorder (AG-1960; Panasonic, Secaucus, NJ). Single frame images were captured from video

tape onto a Macintosh Quadra 950 (Apple Computer, Cupertino, CA) using NIH Image software.

Quantitation of organelle and bead motility was accomplished by counting the number of vesicle, membrane tubule, or bead movements per min on astral microtubules. If an organelle or bead moved, then paused for more than 2 s, and then moved again at some later time, it was scored as two movements. Recordings of motility were done on centrosome-nucleated microtubule asters of comparable size and microtubule density. These asters enabled the directionality of motility to be determined, since all microtubule minus ends are located at the center. The polarity of these astral microtubule arrays was confirmed by a motility assay using kinesin-coated 0.2-μm carboxylated beads.

Polyacrylamide Gel Electrophoresis and Immunoblotting

Protein samples were separated on either 5, 4–15, or 5–15% gradient polyacrylamide gels under denaturing and reducing conditions (Laemmli, 1970). Immunoblotting (Towbin et al., 1979) was performed by electroblotting to nitrocellulose membranes at 0.2 A for 1 h for 5% gels and 0.3 A for 1 h for 5–15% gels. Primary antibodies and dilutions (overnight at 4°C unless indicated): *Dictyostelium* dynein heavy chain (1:5,000 dilution) from Mike Koonce, Wadsworth Center for Laboratories and Research, Albany, NY (Koonce et al., 1992); chicken dynein intermediate chain mAb 70.1 (Steuer et al., 1990) (1–2 h at 22°C at 1:2,000 dilution); chicken dynein light intermediate chain antibody (Gill et al., 1994) from Trina Schroer (Johns Hopkins University, Baltimore, MD) (1:500 dilution); human ubiquitous kinesin heavy chain polyclonal antibody (Niclas et al., 1994) (1:500 dilution); chicken $p150^{Glued}$ mAb 150B from Trina Schroer (1:250 dilution); rat $p150^{Glued}$ polyclonal antibodies UP235 and UP236 (Melloni et al., 1995) from Erica Holzbaur (University of Pennsylvania, Philadelphia, PA) and Dart and Port from Richard Vallee, (Worcester Foundation, Shrewsbury, MA) (1:500-fold dilution); actin mAb AC-40 (Sigma Chemical Co., St. Louis, MO) (1:500 dilution); anti-Arp1/centractin UP454 from Erica Holzbaur (1:250 dilution). Blots were then washed and treated for 1 h at 22°C with either HRP-conjugated (Amersham Corp., Arlington Heights, IL) or alkaline phosphatase–conjugated secondary antibodies (Jackson Immunoresearch Laboratories, West Grove, PA). For confirmation of quantitative differences of membrane-bound dynein between interphase and metaphase extracts, some immunoblots were also performed with an ^{35}S-labeled sheep anti–mouse secondary antibody (Amersham Corp.) used at 0.5 μCi/ml. Blots were developed using the ECL Western blotting detection kit (Amersham Corp.) and exposed to either Kodak XAR-5 film (Eastman Kodak, Rochester, NY), Hyperfilm-ECL (Amersham Corp.), or phosphorImaging screens. Quantitative analysis of bands on films was done either by scanning with a UMAX Power Look PS-2400X (UMAX Data Systems, Inc., Industrial Park, Hsinchu, Taiwan) and then importing the image into the NIH Image software (Wayne Rasband, National Institutes of Health) for densitometric analysis or by phosphorimage analysis with a molecular imager system (GS-363; Bio-Rad Laboratories, Richmond, CA) (for ECL) or by using a phosphorImager (BAS 2000; Fuji Photo Film Co., Tokyo, Japan) (for ^{35}S). Serial dilutions of immunoblot samples were used to select bands within the linear range for quantitation.

Purification of Frog Egg Cytoplasmic Dynein

4 ml crude interphase frog extract (S1) were diluted with 8 ml BRB80 (80 mM K-Pipes, pH 6.8, 1 mM $MgCl_2$, 1 mM EGTA) containing *Xenopus* protease inhibitors, 0.1 mM PMSF, and 1 mM DTT. A high speed supernatant (S2) was made by centrifugation at 109,000 g_{max} for 30 min at 2°C in a Beckman TLA-100.4 rotor. To the S2, taxol was added to 20 μM and prepolymerized bovine brain microtubules were added to 100 μg/ml. After 20 min at 22°C, apyrase was added to 1 U/ml and AMP-PNP to 0.2 mM, and S2 was incubated another 20 min at 22°C. The nucleotide-depleted S2 was then loaded onto a 20% sucrose cushion (BRB80, 4 μM taxol, 1 mM DTT, *Xenopus* protease inhibitors) and spun at 87,000 g_{max} for 10 min at 25°C (TLA 100.4 rotor). The microtubule-depleted supernatant (S3) was removed and the pellet resuspended in 0.8 ml BRB80 (4 μM taxol, 1 mM DTT, and *Xenopus* protease inhibitors). The resuspended microtubules were spun at 87,000 g_{max} for 10 min at 25°C through a 20% sucrose cushion again. The supernatant (MT wash) was removed and the pellet resuspended in 0.2 ml BRB80 (4 μM taxol, 1 mM DTT, and *Xenopus* protease inhibitors) plus 10 mM Mg-ATP followed by a 20-min incubation at 22°C. The microtubules were then pelleted by spinning at 70,000 g_{max} and the supernatant collected (ATP release). The ATP release was then loaded onto a 2.2-ml 5–25% sucrose gradient (*Xenopus* protease inhibitors, 1 mM DTT, 0.1 mM Mg-ATP) and spun at 2°C for 3 h at 259,000 g_{max} (TLS-55 rotor). 0.2-ml fractions were collected, and the dynein peak was determined by running the fractions on a polyacrylamide gel and Coomassie staining. The dynein peak fraction was kept on ice for the dynein addback experiment.

Phosphorylation of Cytoplasmic Dynein in Extracts

A pool of radiolabeled ATP was obtained by adding [^{32}P]orthophosphate to extracts, and labeled cytoplasmic dynein was then isolated either by immunoprecipitation or by microtubule affinity followed by sucrose density gradient centrifugation.

For immunoprecipitation experiments, 20 μl extract was preincubated with cyclinΔ90 or water for 30 min at 22°C, after which 100 μCi [^{32}P]orthophosphate was added and the incubation continued for 30 min. The labeling was stopped by adding 1 ml of ice-cold IP buffer (10 mM Tris, 80 mM sodium β-glycerophosphate, 10 mM sodium pyrophosphate, pH 7.5, plus 1% Triton X-100 and protease inhibitors) and incubating on ice for 10 min. All subsequent procedures were carried out at 4°C. After a clarifying spin at 13,000 g_{max} in a microfuge, half the supernatant was incubated with 2.5 μl mAb 70.1 ascites for 1–2 h, while the other half served as a minus antibody control. Anti–mouse IgM agarose beads (obtained from Sigma Chemical Co.) were then added (15 μl packed beads/sample), and the incubation continued for 1–2 h. The beads were then washed 4× with IP buffer, once with IP buffer plus 500 mM NaCl, and finally once with 50 mM Tris (pH 7.5). Pellets were resuspended in sample buffer and analyzed on 4–15% SDS-PAGE gels. After staining with colloidal Coomassie (Sigma Chemical Co.), the gels were dried and exposed to imaging plates (BAS-III; Fuji Photo Film Co.) or film (Biomax; Eastman Kodak). Quantitation of labeled bands was performed on a phosphorImager (BAS-2000; Fuji Photo Film Co.). To correct for differences in loading, the amount of Coomassie-stained cytoplasmic dynein heavy chains was determined by digitizing the bands using a scan jet (IIcx/T; Hewlett-Packard Co., Palo Alto, CA) followed by analysis using NIH image software.

Microtubule affinity was used as an alternative method for purifying labeled cytoplasmic dynein. 100-μl extracts were preincubated with cyclin Δ90 or water for 20 min, supplemented with 200 μCi [^{32}P]orthophosphate per sample, and then incubated for a further 40 min at room temperature. Labeled extracts were diluted with 220 μl buffer A (120 mM sodium β-glycerophosphate, 15 mM sodium pyrophosphate, 15 mM Hepes, 15 mM EGTA, 7.5 mM $MgCl_2$, pH 7.4) containing 1 mM DTT, protease inhibitors, 10 μg/ml cytochalasin D, and 1.5 μM microcystin. The microtubule affinity protocol was performed as described above except that bovine brain microtubules were used at 150 μg/ml, and hexokinase and AMP-PNP were used at 10 U/ml and 0.4 mM, respectively. In addition, BRB80 was replaced in all subsequent steps by buffer B (buffer A diluted 1.5×, plus 4 μM taxol, 1 mM DTT, protease inhibitors, 1 μg/ml cytochalasin D, 1 μM microcystin). The motor fraction was then loaded onto 600 μl 10–25% sucrose gradients (in 25 mM K-Pipes, 1 mM $MgCl_2$, 1 mM EGTA, pH 6.8, plus 1 mM DTT, protease inhibitors, 100 nM microcystin) and centrifuged in an SW50 rotor with adapters for 5 h at 200,000 g_{max}, 4°C. 50-μl fractions were collected from the top of the gradient and were analyzed as for the immunoprecipitates, except that the gels were silver stained.

Results

Dynein is a Minus End Organelle Motor in Xenopus Eggs

Extracts from *Xenopus* eggs have been shown to promote high levels of minus end microtubule–based organelle transport (Allan and Vale, 1991). To determine if cytoplasmic dynein drives minus end organelle transport in the *Xenopus* egg, we examined whether retrograde motility is eliminated after biochemically inactivating this motor by UV–vanadate photocleavage as described in prior studies (Schnapp and Reese, 1989; Schroer et al., 1989). To assay organelle transport activity, high speed supernatants were combined with purified crude membrane fractions and the directionality of membrane transport (both vesicles and

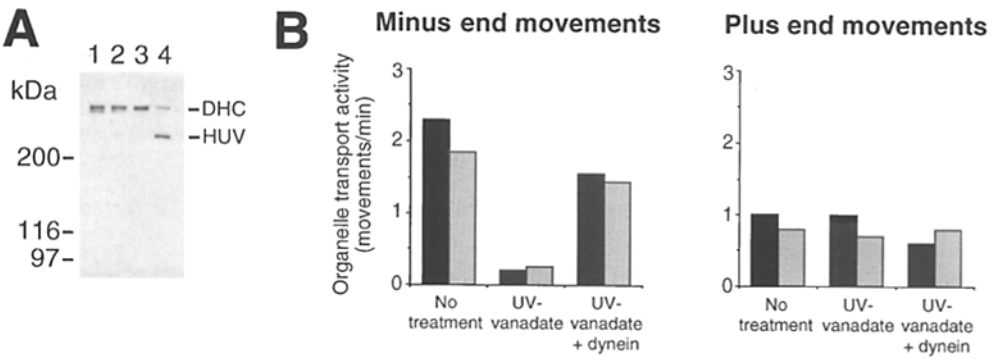

Figure 1. Role of cytoplasmic dynein in minus end–directed membrane transport in *Xenopus* egg extracts. (*A*) UV–vanadate photocleavage of cytoplasmic dynein in *Xenopus* egg extracts. Samples of crude interphase egg extracts containing 2 mM ATP, 5 mM Mg-acetate, and 2 mM DTT were incubated for 1 h on ice under the following conditions. Lane *1*, no UV irradiation or vanadate; lane *2*, UV irradiation only; lane *3*; 20 μM vanadate only; lane *4*, UV irradiation and 20 μM vanadate. 100 μg of each sample was run on a 5% polyacrylamide gel, transferred to nitrocellulose, and then probed with an anti-*Dictyostelium* dynein heavy chain polyclonal antibody that only recognizes the larger of the two photocleavage products (Lee-Eiford et al., 1986; Gibbons et al., 1987). 85% of the dynein heavy chain was photocleaved into two smaller fragments by UV and vanadate, whereas incubation with either UV irradiation or vanadate alone did not lead to any detectable cleavage. Molecular mass standards (*kD*) are shown on the left side. The dynein heavy chain (*DHC*) and the larger heavy chain photocleavage product (*HUV*) are indicated on the right side. UV–vanadate photocleavage appears to be specific for dynein, since the kinesin heavy chain was immune to photocleavage even at orthovanadate concentrations as high as 100 μM (data not shown). (*B*) Restoration of minus end–directed transport to UV photocleaved extracts by addition of purified *Xenopus* egg dynein. Data from two different experiments are shown. Final concentrations of supernatant, organelles, and dynein were ~7, 2, and 0.02 mg/ml, respectively. 20-min assays were recorded for each sample and plus end– and minus end–directed organelle movements were scored.

membrane tubules [Allan and Vale, 1991]) was scored on microtubules polymerized from *Spisula* egg centrosome particles (Palazzo et al., 1992). UV–vanadate treatment of the extract cleaved 85% of the dynein heavy chain (Fig. 1 *A*), which resulted in a 81% decrease in minus end transport of vesicles and membrane tubules in comparison to the untreated control but had little effect on plus end–directed motility (Table I). UV or vanadate (8 μM final concentration) alone had little effect on motility in either direction, indicating that the reduction of motility was due to photocleavage. Similar results were also seen using 0.2-μm carboxylated beads, suggesting that they were also transported by dynein (Table I). To establish that UV inhibition of membrane transport was due to dynein cleavage, egg cytoplasmic dynein was purified and added back to the UV–vanadate photocleaved extract. Readdition of dynein restored the level of minus end motility to within ~30% of control levels in two different assays but did not increase the amount of plus end motility (Fig. 1 *B*). Hence, dynein is responsible for the minus end transport of most, if not all, of the vesicles and membrane tubules in the cytoplasm of the *Xenopus* egg.

Dynein Dissociates from Membranes in Metaphase Extracts

Previous studies have shown that both minus end– and plus end–directed microtubule-based organelle transport are dramatically inhibited in metaphase extracts in comparison to interphase extracts (Allan and Vale, 1991). However, minus end motility of microtubules along glass and beads along microtubules in metaphase extracts still occurred. Moreover, UV–vanadate treatment of mitotic high speed supernatants dramatically reduced minus end bead motility (1.6 ± 0.3 movements/min compared with 38.3 ± 4.5 movements/min for the vanadate only control; $n = 3$), which indicates that dynein is the predominant soluble minus end–directed motor in mitotic extracts. This result suggests that the motor domain of soluble dynein is still active in mitosis and that either the motor activity of membrane-bound dynein is selectively inactivated or that dynein dissociates from membranes in mitotic extracts.

To distinguish between the two possibilities described above, the relative quantities of dynein attached to purified total cytosolic membranes isolated from interphase- and metaphase-arrested extracts were examined. Interphase-arrested extracts were made from eggs that were electrically activated, and cycloheximide was included to inhibit cyclin synthesis. Metaphase extracts were prepared by treating the interphase extract with cyclinΔ90, a nondegradable form of cyclin B that activates $p34^{cdc2}$ kinase (Murray et al., 1989). H1 kinase assays were used to demonstrate conversion of interphase extracts to metaphase (Fig. 2 *A*). Crude membrane fractions were prepared by flotation through a sucrose step gradient (see Materials and Methods), and equal amounts of interphase and

Table I. Organelle and Bead Transport in UV–Vanadate Photocleaved Interphase Xenopus Egg Extracts

	Minus-end directed		Plus-end directed	
	Organelles (vesicles and tubules)	Beads	Organelles (vesicles and tubules)	Beads
	movements/min		*movements/min*	
No treatment	4.52 ± 0.76	27.0 ± 3.76	0.63 ± 0.07	2.87 ± 0.67
UV	3.59 ± 0.23	22.3 ± 3.76	0.61 ± 0.10	2.53 ± 0.35
Vanadate	4.11 ± 1.12	29.4 ± 4.48	0.51 ± 0.12	3.17 ± 1.3
UV-vanadate	0.88 ± 0.07	4.8 ± 1.39	0.60 ± 0.09	1.23 ± 0.15

High speed supernatants and isolated membranes were prepared from the four extract samples described in Fig. 1. 8 μl high speed supernatant (14.4 mg/ml), 2 μl membranes (10 mg/ml), or 2 μl carboxylated beads (1:40 dilution) and 0.5 μl 20× ATP regeneration system were combined, applied to microtubule asters, and assessed for minus end– and plus end–directed motility. For each condition, motility data were analyzed from three separate slide chambers in which one centrosome was observed for 30 min in each (means ± SD are shown). Data in this table are representative of two experiments.

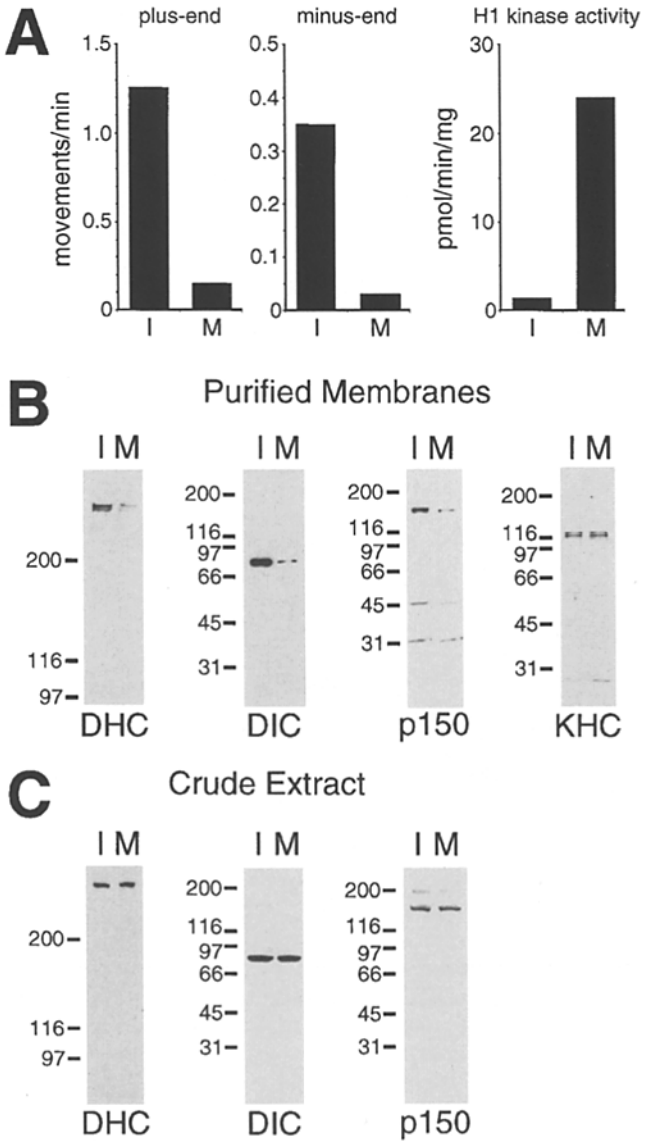

Figure 2. Minus end–directed motility and association of dynein with cytosolic membranes decrease in parallel in metaphase versus interphase extracts. (*A*) Minus end– and plus end–directed organelle motility was scored by combining 5 μl of interphase or metaphase high speed supernatant (16.5 mg/ml) with 5 μl isolated interphase or metaphase total membrane (2.5 mg/ml), respectively, and 0.5 μl of a 20× ATP regenerating system. Levels (organelle movements/min) and directionality (minus or plus) of transport of vesicles and membrane tubules were assessed on centrosome-nucleated microtubule asters. Histone H1 kinase assays were used to assess the cell cycle state of interphase and metaphase extracts. Units of activity are expressed as pmol/min/mg of protein. (*B*) Immunoblots of equal loadings (40 μg for all cases except p150^{Glued} which had 150 μg) of isolated interphase (*I*) and metaphase (*M*) membranes were probed with antibodies directed against either dynein heavy chain (*DHC*), dynein intermediate chain (*DIC*), p150^{Glued} (*p150*), or kinesin heavy chain (*KHC*). (*C*) Immunoblots of equal loadings (160 μg) of crude interphase and metaphase extracts were probed with anti-dynein heavy chain (*DHC*) and intermediate chain (*DIC*) antibodies as well as an anti-p150^{Glued} antibody to show that the total amounts of dynein and p150^{Glued} in interphase and metaphase extracts are the same. For the p150^{Glued} immunoblots, the UP235 antibody was used. Other anti-p150^{Glued} antibodies (see Materials and Methods) yielded identical results. Molecular mass standards (*kD*) are shown on the left sides of the immunoblots.

metaphase membranes were then subjected to electrophoresis and immunoblotting. Densitometric analysis of the immunoblots revealed that interphase membranes contained an average of 6.5 ± 0.75-fold (mean ± SD; $n = 3$) more dynein heavy chain compared with metaphase membranes. Similar immunoblotting experiments performed with a dynein intermediate chain antibody revealed an average 7.2 ± 2.0-fold ($n = 3$) more dynein on interphase compared with metaphase membranes (Fig. 2 *B*). p150^{Glued} of the dynactin complex, which has been shown to stimulate dynein-based organelle transport (Gill et al., 1991), was also similarly reduced (6.3 ± 1.2-fold; $n = 3$) in metaphase compared with interphase membranes. In contrast, there was no difference in the amount of kinesin heavy chain associated with membranes from these two cell cycle states. To rule out the possibility that dynein and p150^{Glued} are being degraded in the metaphase state, crude interphase and metaphase extracts were probed with anti-dynein heavy or intermediate chain antibodies or an anti-p150^{Glued} antibody. No change in the levels of the dynein heavy or intermediate chains or p150^{Glued} were found when comparing these two cell cycle states (Fig. 2 *C*).

The differences in association of dynein with membranes correlated with the reduction in minus end organelle motility seen in the same extracts used for the isolation of membrane for immunoblotting. As shown in Fig. 2 *A*, minus end motility was reduced eightfold in the metaphase extract when compared with the interphase extract, consistent with previous findings (Allan and Vale, 1991). Transport of both membrane tubules and vesicles were similarly decreased. These results strongly suggest that cytoplasmic dynein–based transport during the cell cycle is controlled by modulating the levels of dynein associated with organelles.

Regulation of Dynein Phosphorylation by the Cell Cycle

As many different examples of cell–cycle dependent regulation are mediated by phosphorylation, we investigated whether dynein is phosphorylated in a cell cycle–dependent manner. When dynein fractions prepared from interphase and metaphase extracts were analyzed by SDS-PAGE and immunoblotting, it was clear that a major dynein-associated polypeptide of ~65 kD underwent a cell cycle–dependent molecular mass shift (67 kD in metaphase versus 62.5 kD in interphase; Fig. 3, *A* and *B*). This polypeptide was identified as a dynein subunit using an antibody to the chicken dynein light intermediate chain (Gill et al., 1994). This subunit was noted previously to migrate more slowly when phosphorylated (Gill et al., 1994; Hughes et al., 1995), suggesting that phosphorylation of this dynein-associated polypeptide chain occurs in metaphase extracts. No change in electrophoretic migration, on the other hand, was observed in the dynein intermediate (~85 kD) or heavy (~500 kD) chains. Since the cytoplasmic dynein was purified from metaphase and interphase extracts in the presence of phosphatase inhibitors to prevent dephosphorylation during the ATP depletion step, it was possible that phosphorylation levels were artificially increased. However, immunoblotting of concentrated metaphase and interphase crude extracts (soluble and membrane compo-

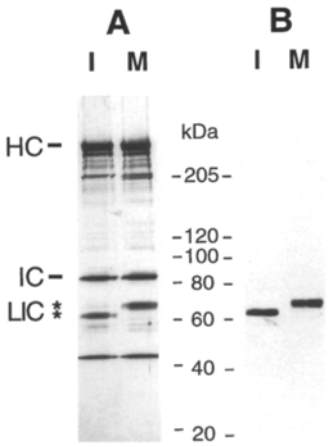

Figure 3. Cell cycle–dependent changes in dynein light intermediate chain apparent molecular weight. Dynein purified from interphase (*I*) and metaphase (*M*) extracts was analyzed by SDS-PAGE and silver staining (*A*), revealing one band which undergoes a substantial shift in apparent M_r (*asterisks*). This component is identified as the major light intermediate chain (*LIC*) by immunoblotting of purified interphase and metaphase dynein (*B*), using a polyclonal anti-light intermediate chain antibody. Molecular mass standards (kD) are given between *A* and *B*, and positions of the dynein heavy (*HC*) and intermediate (*IC*) chains are also indicated. Note: one unexpected finding was that preparing the dynein in the presence of phosphatase inhibitors drastically reduced the amount of the $p150^{Glued}$ component of dynactin present in the dynein gradient fractions to levels that were undetectable by silver staining. In addition, centractin/Arp1 levels were very low in these fractions, as detected by immunoblotting, although contaminating conventional actin was present (data not shown). This also makes it highly unlikely that the 67- and 62.5-kD region of the gels also contain components of the dynactin complex.

nents) solubilized directly into gel sample buffer revealed an identical increase in apparent molecular weight in metaphase versus interphase light intermediate chains (data not shown). Furthermore, all of the detectable dynein light intermediate chain was in the 67- and 62.5-kD forms in mitotic and interphase crude extracts, respectively.

Incorporation of phosphate into the dynein molecule was assayed directly by incubating metaphase and interphase extracts with [^{32}P]orthophosphate to generate a pool of [^{32}P]γ-ATP, which then serves as a substrate for endogenous kinases. When dynein was immunoprecipitated (Fig. 4 *A*), a prominently phosphorylated band of ~67 kD was observed in metaphase extracts (lane *M*+), that was not detected in the absence of antibody (lane *M*−). In interphase, a band of slightly lower M_r (62,500) was phosphorylated (not readily seen in Fig. 4 *A*), but to a much lesser extent. These molecular weights correspond well to those of the dynein light intermediate chains in metaphase and interphase described above, but this could not be confirmed by comparison with total protein composition of the immunoprecipitates due to comigrating antibody bands. Quantitation of the labeled bands from phosphorImager data (with standardization for the amount of Coomassie-stained heavy chain) revealed that 11.5 ± 2.6-fold (n = 3) more [^{32}P]phosphate was incorporated into the dynein light intermediate chain in metaphase versus inter-

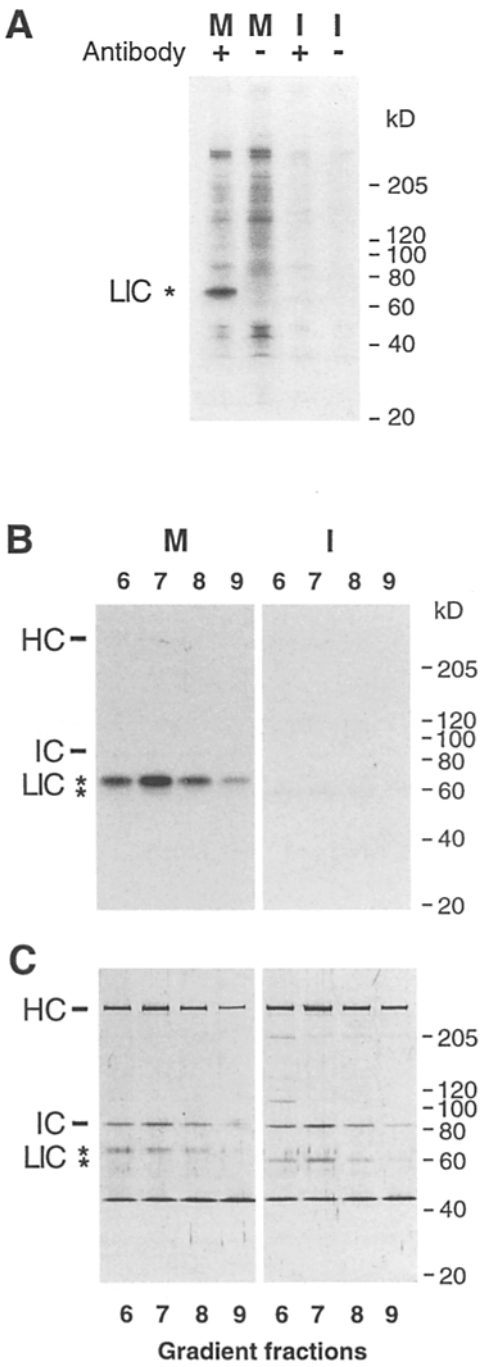

Figure 4. Cell cycle–dependent phosphorylation of dynein light intermediate chain. (*A*) Metaphase (*M*) and interphase (*I*) extracts were incubated with [^{32}P]orthophosphate as described in Materials and Methods, and then cytoplasmic dynein was immunoprecipitated using 70.1, an intermediate chain mAb (lanes +), with omission of the antibody as controls (lanes −). Autoradiography revealed a 67-kD band (*LIC*) that was strongly labeled in metaphase. Molecular mass standards (*kD*) are shown. (*B* and *C*) Cell cycle–dependent phosphorylation of dynein light intermediate chain in dynein isolated by microtubule affinity and sucrose density gradient centrifugation (see Materials and Methods). Four adjacent fractions (from bottom to top of gradient: 6, 7, 8, and 9) containing the dynein peak are shown, with phosphorylated protein detected by autoradiography (*B*) and total protein revealed by silver staining (*C*). (*Left panels, metaphase; right panels, interphase*). Again, phosphate was strongly incorporated in metaphase into a 67-kD band that comigrated with the light intermediate chain. The position of dynein heavy (*HC*), intermediate (*IC*), and light intermediate (*LIC*) chains are shown, with asterisks indicating the two molecular weight forms of the light intermediate chain. Molecular mass standards (*kD*) are also shown.

phase. All other labeled polypeptides were also observed in the minus antibody controls. Quantitation of other dynein polypeptides by Coomassie staining and immunoblotting revealed that immunoprecipitations brought down equal amounts of both the dynein heavy and intermediate chains from interphase and mitotic extracts (interphase/metaphase ratio of 1.08 and 1.04 for the heavy and intermediate chains, respectively). Since these polypeptides were not heavily labeled with [^{32}P]phosphate, neither the heavy nor intermediate dynein chains appear to undergo significant phosphate turnover in either mitotic or interphase extract.

To confirm that the 67-kD phosphorylated band was indeed the light intermediate subunit, dynein was isolated from labeled extracts by microtubule affinity and sucrose density gradient centrifugation. Again, a prominent labeled band of 67 kD was observed in metaphase dynein (Fig. 4 *B*, *left*), which comigrated with the light intermediate chain (Fig. 4 *C*, *left*). Autoradiography of interphase dynein (Fig. 4 *B*, *right*) revealed a polypeptide of 62.5 kD which comigrated with the interphase light intermediate chain (Fig. 4 *C*, *right*), and which had incorporated 13.1-fold less [^{32}P]phosphate than the metaphase light intermediate chain. A high M_r polypeptide in both metaphase and interphase gradients also contained a low level of phosphate, but the peak of this labeled species across the gradient did not coincide with the dynein heavy chain (data not shown).

Taken together, these data indicate that both the turnover of phosphate in the light intermediate chain and the steady state phosphate levels (as shown by the increased apparent molecular weight of the light intermediate chain in Fig. 3) are considerably higher in metaphase compared with interphase.

Discussion

In this study, we have examined the mechanism by which organelle transport is regulated by the cell cycle in extracts of *Xenopus* eggs. Previous work by Allan and Vale (1991) documented a profound inhibition of minus end–directed membrane motility when an interphase extract was converted to a metaphase state. Here, we have shown that cytoplasmic dynein is the predominant, if not sole, motor that drives minus end–directed organelle transport and have found that the amounts of dynein and its activator dynactin that are bound to membranes decrease approximately sevenfold when extracts enter metaphase. The magnitude of this decrease in membrane-associated dynein is very similar to the reduction in minus end–directed organelle transport observed in the same metaphase extract. Thus, modulation of dynein association with membranes appears to provide an explanation for how minus end–directed organelle transport is controlled by the cell cycle.

Regulation of both dynein association with membranes and dynein-based organelle transport must be mediated by a posttranslational event, since the cell cycle state of extracts can be interconverted in the presence of protein synthesis inhibitors. Although a previous study did not detect any phosphorylation of dynein in crude interphase and metaphase motor fractions (Verde et al., 1991), we detected substantial phosphorylation of the light intermediate chain of dynein isolated from metaphase extracts by either immunoprecipitation or microtubule affinity and velocity sedimentation. The increase in the turnover and steady-state levels of radiolabeled phosphate into this ~67-kD light intermediate chain in metaphase compared with interphase extracts is similar to the magnitude of the changes observed in organelle transport and dynein association with membranes. In contrast, the heavy and intermediate chains incorporated very little radiolabeled phosphate, and labeling did not change in a cell cycle–dependent manner. These findings suggest that light intermediate chain phosphorylation may be responsible for decreasing the affinity of dynein for membranes, although phosphorylation of additional proteins might also be involved.

Previous studies have correlated cytoplasmic dynein heavy chain phosphorylation with changes in dynein localization (Lin et al., 1994) and possibly motor activity (Dillman and Pfister, 1994). Here we show that light intermediate chain phosphorylation may be involved in altering the cargo-binding activity of dynein. The group of dynein intermediate chains have been considered to be strong candidates for targeting this motor to subcellular structures. In the case of flagellar dynein, the intermediate chains may be responsible for anchoring the motor to the A-microtubules of the axoneme (Mitchell and Rosenbaum, 1986; King and Witman, 1990; King et al., 1991), while the intermediate and light intermediate chains have been speculated to serve a similar function in docking cytoplasmic dynein to intracellular targets (Paschal et al., 1992; Gill et al., 1994; Hughes et al., 1995). The binding partners of the light intermediate chain are unknown, while the intermediate chain has been shown to dock cytoplasmic dynein to the p150^{Glued} subunit of the dynactin complex (Karki and Holzbaur, 1995; Vaughan and Vallee, 1995). Whether the phosphorylation of light intermediate chains affects this interaction is an interesting topic for further investigation.

Light intermediate chain phosphorylation may be responsible, at least in part, for the different roles of dynein during the cell cycle. Some studies have shown that dynein changes its location from a vesicular staining pattern in interphase to spindle and kinetochore staining in mitosis (Pfarr et al., 1990; Steuer et al., 1990). A reduction in the role of dynein in vesicle transport in mitosis is also consistent with lack of Golgi association with microtubules and the decrease in membrane-trafficking events during mitosis (Warren et al., 1984; Warren and Wickner, 1996). Furthermore, various studies have provided clear evidence that dynein is involved in mitotic spindle formation, (Vaisberg et al., 1993), spindle orientation and nuclear segregation (Eshel et al., 1993; Li et al., 1993; Plamann et al., 1994; Xiang et al., 1994), and chromosome segregation (Saunders et al., 1995). Therefore, the dissociation of cytoplasmic dynein from membranes described here may allow this motor to bind to new cargo and perform distinct roles during metaphase.

This is the first study in which cell cycle–dependent dynein phosphorylation and dynein-based organelle transport have been directly measured in the same system. However, other studies have indirectly suggested a possi-

ble connection between dynein phosphorylation and organelle transport in interphase cells that differs from the results described here. In interphase *Xenopus* egg extracts, okadaic acid increases minus end–directed ER membrane tubule motility without changing the levels of membrane-associated dynein (Allan, 1995). Whether this activation is due to increased dynein phosphorylation has not been directly shown. In addition, studies in the rat optic nerve suggest that phosphorylation of dynein may stimulate membrane transport, since dynein heavy chain phosphorylation is higher on retrograde versus anterograde-moving organelles (Dillman and Pfister, 1994).

Our findings can be reconciled with the above studies by proposing that dynein-based transport can be regulated through membrane attachment as well as the activity of the motor domain. Moreover, interphase and metaphase dynein regulation may be distinct and operate primarily through diffferent dynein subunits. The data presented here suggest that kinases active during metaphase phosphorylate the dynein light intermediate chain, resulting in detachment from membranes and decreased organelle transport. The microtubule-translocating activity of the motor domain, however, appears to be unaltered, based on latex bead motility assays shown here and in previous studies (Allan and Vale, 1991). In contrast, dynein heavy chain phosphorylation may be the primary mechanism for regulating activity in interphase (Dillman and Pfister, 1994; Lin et al., 1994). The effects of dynein phosphorylation, however, may also depend on the cell type. As an example, okadaic acid treatment of interphase *Xenopus* extract causes a dramatic increase in ER tubule transport without affecting the association of dynein with membranes (Allan, 1995), while application of this phosphatase inhibitor to fibroblasts causes dissociation of dynein from intracelluar membranes (Lin et al., 1994).

Plus end–directed motility in *Xenopus* extracts is also suppressed in metaphase extracts when compared with interphase extracts. A likely candidate for a motor mediating at least a portion of the plus end–directed motility is kinesin. Unlike dynein, levels of this motor on membranes isolated from interphase and metaphase extracts are the same, suggesting that kinesin may be regulated in a different manner than dynein. Further work is required to establish whether plus end–directed organelle transport is regulated by controlling the force-generating activity of kinesin or whether other plus end–directed motors drive organelle transport in the *Xenopus* egg.

We thank Dr. Robert Palazzo for the aster-forming *Spisula* extract and advice on their use, Drs. Frank McNally and Paul Clarke for the cyclinΔ90, and Drs. Trina Schroer, Mike Koonce, Richard McIntosh, Erica Holzbaur, and Richard Vallee for providing antibodies. We are also grateful to Dr. Ian Gibbons for advice on the UV–vanadate photocleavage technique, Dr. Colin Stirling for advice on phosphorimaging and image transfer, and Arshad Desai for providing comments on the manuscript.

This work was supported by grants from the Medical Scientist Training Program (National Institutes of Health) and the University of California Chancellor's Fellowship (both to J. Niclas) and the National Institutes of Health (to R.D. Vale). V. Allan is a Lister Fellow and her work was supported by the Lister Institute and the Royal Society.

Received for publication 30 August 1995 and in revised form 8 March 1996.

References

Allan, V. 1995. Protein phosphatase 1 regulates the cytoplasmic dynein–driven formation of endoplasmic reticulum networks in vitro. *J. Cell Biol.* 128:879–891.

Allan, V.J., and R.D. Vale. 1991. Cell cycle control of microtubule-based membrane transport and tubule formation in vitro. *J. Cell Biol.* 113:347–359.

Brady, S.T. 1985. A novel brain ATPase with properties expected for the fast axonal transport motor. *Nature (Lond.).* 317:73–75.

Dillman, J.F.R., and K.K. Pfister. 1994. Differential phosphorylation in vivo of cytoplasmic dynein associated with anterogradely moving organelles. *J. Cell Biol.* 127:1671–1681.

Eshel, D., L.A. Urrestarazu, S. Vissers, J.C. Jauniaux, J.C. van Vliet-Reedijk, R.J. Planta, and I.R. Gibbons. 1993. Cytoplasmic dynein is required for normal nuclear segregation in yeast. *Proc. Natl. Acad. Sci. USA.* 90:11172–11176.

Echeverri, C.J., B.M. Paschal, K.T. Vaughan, and R.B. Vallee. 1996. Molecular characterization of the 50-kD subunit of dynactin reveals function for the complex in chromosome alignment and spindle organization during mitosis. *J. Cell Biol.* 132:617–633.

Gibbons, I.R., A. Lee-Eiford, G. Mocz, C.A. Phillipson, W. Tang, and B.H. Gibbons. 1987. Photosensitized cleavage of dynein heavy chains. Cleavage at the "V1 site" by irradiation at 365 nm in the presence of ATP and vanadate. *J. Biol. Chem.* 262:2780–2786.

Gill, S.R., D.W. Cleveland, and T.A. Schroer. 1994. Characterization of DLC-A and DLC-B, two families of cytoplasmic dynein light chain subunits. *Mol. Biol. Cell.* 5:645–654.

Gill, S.R., T.A. Schroer, I. Szilak, E.R. Steuer, M.P. Sheetz, and D.W. Cleveland. 1991. Dynactin, a conserved, ubiquitously expressed component of an activator of vesicle motility mediated by cytoplasmic dynein. *J. Cell Biol.* 115:1639–1650.

Hamm-Alvarez, S.F., Y.K. Preston, and M.P. Sheetz. 1993. Regulation of vesicle transport in CV-1 cells and extracts. *J. Cell Sci.* 106:955–966.

Hollenbeck, P.J. 1993. Phosphorylation of neuronal kinesin heavy and light chains in vivo. *J. Neurochem.* 60:2265–2275.

Hollenbeck, P.J., and J.A. Swanson. 1990. Radial extension of macrophage tubular lysosomes supported by kinesin. *Nature (Lond.).* 346:864–866.

Hughes, S.M., K.T. Vaughan, J.S. Herskovits, and R.B. Vallee. 1995. Molecular analysis of a cytoplasmic dynein light intermediate chain reveals homology to a family of ATPases. *J. Cell Sci.* 108:17–24.

Karki, S., and E.L. Holzbaur. 1995. Affinity chromatography demonstrates a direct binding between cytoplasmic dynein and the dynactin complex. *J. Biol. Chem.* 270:28806–28811.

King, S.M., and G.B. Witman. 1990. Localization of an intermediate chain of outer arm dynein by immunoelectron microscopy. *J. Biol. Chem.* 265:19807–19811.

King, S.M., C.G. Wilkerson, and G.B. Witman. 1991. The M_r 78,000 intermediate chain of *Chlamydomonas* outer arm dynein interacts with α-tubulin in situ. *J. Biol. Chem.* 266:8401–8407.

Koonce, M.P., P.M. Grissom, and J.R. McIntosh. 1992. Dynein from *Dictyostelium*: primary structure comparisons between a cytoplasmic motor enzyme and flagellar dynein. *J. Cell Biol.* 119:1597–1604.

Kotz, K.J., and M.A. McNiven. 1994. Intracellular calcium and cAMP regulate directional pigment movements in teleost erythrophores. *J. Cell Biol.* 124: 463–474.

Laemmli, U.K. 1970. Cleavage of structural proteins during assembly of the head of bacteriophage T4. *Nature (Lond.)* 227:680–685.

Lee, K.D., and P.J. Hollenbeck. 1995. Phosphorylation of kinesin in vivo correlates with organelle association and neurite outgrowth. *J. Biol. Chem.* 270: 5600–5605.

Lee-Eiford, A., R.A. Ow, and I.R. Gibbons. 1986. Specific cleavage of dynein heavy chains by ultraviolet irradiation in the presence of ATP and vanadate. *J. Biol. Chem.* 261:2337–2342.

Li, Y.Y., E. Yeh, T. Hays, and K. Bloom. 1993. Disruption of mitotic spindle orientation in a yeast dynein mutant. *Proc. Natl. Acad. Sci. USA.* 90:10096–10100.

Lin, S.X., K.L. Ferro, and C.A. Collins. 1994. Cytoplasmic dynein undergoes intracellular redistribution concomitant with phosphorylation of the heavy chain in response to serum starvation and okadaic acid. *J. Cell Biol.* 127: 1009–1019.

Lynch, T.J., J.D. Taylor, and T.T. Tchen. 1986*a*. Regulation of pigment organelle translocation. I. Phosphorylation of the organelle-associated protein p57. *J. Biol. Chem.* 261:4204–4211.

Lynch, T.J., B.Y. Wu, J.D. Taylor, and T.T. Tchen. 1986*b*. Regulation of pigment organelle translocation. II. Participation of a cAMP-dependent protein kinase. *J. Biol. Chem.* 261:4212–4216.

Matthies, H.J., R.J. Miller, and H.C. Palfrey. 1993. Calmodulin binding to and cAMP-dependent phosphorylation of kinesin light chains modulate kinesin ATPase activity. *J. Biol. Chem.* 268:11176–11187.

McIlvain, J.M., Jr., J.K. Burkhardt, S. Hamm-Alvarez, Y. Argon, and M.P. Sheetz. 1994. Regulation of kinesin activity by phosphorylation of kinesin-associated proteins. *J. Biol. Chem.* 269:19176–19182.

Melloni, R.H., M.K. Tokito, and E.L. Holzbaur. 1995. Expression of the p150 glued component of the dynactin complex in developing and adult brain. *J. Comp. Neurol.* 357:15–24.

Mitchell, D.R., and J.L. Rosenbaum. 1986. Protein-protein interactions in the 18S ATPase of *Chlamydomonas* outer dynein arms. *Cell Motil. Cytoskeleton.* 6:510–520.

Muhua, L., T.S. Karpova, and J.A. Cooper. 1994. A yeast actin-related protein homologous to that in vertebrate dynactin complex is important for spindle orientation and nuclear migration. *Cell.* 78:669–679.

Murray, A.W. 1991. Cell cycle extracts. *Methods Cell Biol.* 36:581–605.

Murray, A.W., M.J. Solomon, and M.W. Kirschner. 1989. The role of cyclin synthesis and degradation in the control of maturation promoting factor activity. *Nature (Lond.).* 339:280–286.

Niclas, J., F. Navone, N. Hom-Booher, and R.D. Vale. 1994. Cloning and localization of a conventional kinesin motor expressed exclusively in neurons. *Neuron.* 12:1059–1072.

Okada, Y., R. Sato-Yoshitake, and N. Hirokawa. 1995. The activation of protein kinase A pathway selectively inhibits anterograde axonal transport of vesicles but not mitochondria transport or retrograde transport in vivo. *J. Neurosci.* 15:3053–3064.

Palazzo, R.E., J.B. Brawley, and L.I. Rebhun. 1988. Spontaneous aster formation in cytoplasmic extracts from eggs of the surf clam. *Zool. Sci. (Tokyo).* 5: 603–611.

Palazzo, R.E., E. Vaisberg, R.W. Cole, and C.L. Rieder. 1992. Centriole duplication in lysates of Spisula solidissima oocytes. *Science (Wash. DC).* 256:219–221.

Paschal, B.M., and R.B. Vallee. 1987. Retrograde transport by the microtubule-associated protein MAP 1C. *Nature (Lond.).* 330:181–183.

Paschal, B.M., H.S. Shpetner, and R.B. Vallee. 1987. MAP 1C is a microtubule-activated ATPase which translocates microtubules in vitro and has dynein-like properties. *J. Cell Biol.* 105:1273–1282.

Paschal, B.M., A. Mikami, K.K. Pfister, and R.B. Vallee. 1992. Homology of the 74-kD cytoplasmic dynein subunit with a flagellar dynein polypeptide suggests an intracellular targeting function. *J. Cell Biol.* 118:1133–1143.

Pfarr, C.M., M. Coue, P.M. Grissom, T.S. Hays, M.E. Porter, and J.R. McIntosh. 1990. Cytoplasmic dynein is localized to kinetochores during mitosis. *Nature (Lond.).* 345:263–265.

Plamann, M., P.F. Minke, J.H. Tinsley, and K.S. Bruno. 1994. Cytoplasmic dynein and actin-related protein Arp1 are required for normal nuclear distribution in filamentous fungi. *J. Cell Biol.* 127:139–149.

Rodionov, V.I., F.K. Gyoeva, and V.I. Gelfand. 1991. Kinesin is responsible for centrifugal movement of pigment granules in melanophores. *Proc. Natl. Acad. Sci. USA.* 88:4956–4960.

Rozdzial, M.M., and L.T. Haimo. 1986. Bidirectional pigment granule movements of melanophores are regulated by protein phosphorylation and dephosphorylation. *Cell.* 47:1061–1070.

Saunders, W.S., D. Koshland, D. Eshel, I.R. Gibbons, and M.A. Hoyt. 1995. *Saccharomyces cerevisiae* kinesin- and dynein-related proteins required for anaphase chromosome segregation. *J. Cell Biol.* 128:617–624.

Schnapp, B.J., and T.S. Reese. 1989. Dynein is the motor for retrograde axonal transport of organelles. *Proc. Natl. Acad. Sci. USA.* 86:1548–1552.

Schroer, T.A., and M.P. Sheetz. 1991. Two activators of microtubule-based vesicle transport. *J. Cell Biol.* 115:1309–1318.

Schroer, T.A., E.R. Steuer, and M.P. Sheetz. 1989. Cytoplasmic dynein is a minus end-directed motor for membranous organelles. *Cell.* 56:937–996.

Steuer, E.R., L. Wordeman, T.A. Schroer, and M.P. Sheetz. 1990. Localization of cytoplasmic dynein to mitotic spindles and kinetochores. *Nature (Lond.).* 345:266–268.

Thaler, C.D., and L.T. Haimo. 1990. Regulation of organelle transport in melanophores by calcineurin. *J. Cell Biol.* 111:1939–1948.

Towbin, J., T. Staehelin, and J. Gordon. 1979. Electrophoretic transfer of proteins from polyacrylamide gels to nitrocellulose sheets: procedure and some applications. *Proc. Natl. Acad. Sci. USA.* 76:4350–4354.

Vaisberg, E.A., M.P. Koonce, and J.R. McIntosh. 1993. Cytoplasmic dynein plays a role in mammalian mitotic spindle formation. *J. Cell Biol.* 123:849–858.

Vale, R.D., T.S. Reese, and M.P. Sheetz. 1985. Identification of a novel force-generating protein, kinesin, involved in microtubule-based motility. *Cell.* 42: 39–50.

Vaughan, K.T., and R.B. Vallee. 1995. Cytoplasmic dynein binds dynactin through a direct interaction between the intermediate chain and $p150^{glued}$. *J. Cell Biol.* 131:1507–1516.

Verde, F., J.M. Berrez, C. Antony, and E. Karsenti. 1991. Taxol-induced microtubule asters in mitotic extracts of Xenopus eggs: requirement for phosphorylated factors and cytoplasmic dynein. *J. Cell Biol.* 112:1177–1187.

Warren, G., and W. Wickner. 1996. Organelle inheritance. *Cell.* 84:395–400.

Warren, G., J. Davoust, and A. Cockcroft. 1984. Recycling of transferrin receptors in A431 cells is inhibited during mitosis. *EMBO (Eur. Mol. Biol. Organ.) J.* 3:2217–2225.

Warren, G., C. Featherstone, G. Griffiths, and B. Burke. 1983. Newly synthesized G protein of vesicular stomatitis virus is not transported to the cell surface during mitosis. *J. Cell Biol.* 97:1623–1628.

Xiang, X., S.M. Beckwith, and N.R. Morris. 1994. Cytoplasmic dynein is involved in nuclear migration in *Aspergillus nidulans*. *Proc. Natl. Acad. Sci. USA.* 91:2100–2104.